Journal of Materials Chemistry A

RSC Publishing

PAPER

View Article Online
View Journal | View Issue

Changes in the electrical resistance of oriented graphitic carbon films induced by atomic hydrogen

Cite this: *J. Mater. Chem. A*, 2013, **1**, 402

Ali Moafi, James G. Partridge,* Abu Z. Sadek and Dougal G. McCulloch

Received 5th September 2012
Accepted 5th October 2012

DOI: 10.1039/c2ta00198e

www.rsc.org/MaterialsA

The electrical resistance of oriented graphitic carbon films supporting catalytic Pt pads decreases upon exposure to hydrogen gas with a magnitude dependent on the crystallographic order in the film. This resistance change is attributed to defects responding to atomic hydrogen spilled over from the catalytic Pt.

Introduction

Due to the worldwide effort to move towards renewable energy sources, hydrogen storage and hydrogen detection have both become important enabling technologies. Carbon based materials have shown great promise in these fields, prompting numerous experimental and theoretical studies.[1,2] However, the mechanisms involved in hydrogen attachment to carbon materials and the effects of hydrogen attachment on the structural/electrical properties of the carbon materials are not yet fully understood.

Conductometric gas sensors have a conductance that changes upon exposure to a target gas. These sensors are frequently used in alarm applications due to their reliability, inherent simplicity, ease of integration with electronic circuits and low cost. Carbon nano-materials including functionalized carbon nanotubes (CNTs)[3,4] and graphene,[5] have been employed as the sensing elements within conductometric gas sensors with good sensitivity,[6–8] low power consumption[7] and response at room temperature.[8] However, they tend to recover slowly after hydrogen exposure.[4,9] Additionally, CNT production/assembly methods can lack compatibility with large-scale device processing due to high temperatures and/or time consuming manipulation/positioning.[10] By comparison, carbon thin films can be deposited using low-cost, scalable physical vapour deposition methods, enabling greater flexibility in device fabrication. Importantly, the chemical, electrical and nano-structural properties of carbon thin films can be altered by controlling the growth conditions.[11,12] Despite this, few reports exist that describe the electrical response of carbon thin films during their exposure to hydrogen.[13]

In the majority of carbon based conductometric hydrogen sensors, catalytic metals such as Pt or Pd are employed to dissociate H_2 into atomic hydrogen. Exposure to hydrogen alters the structural and electrical properties of the catalytic metal, providing a measurable response.[14] In a process commonly referred to as "hydrogen spillover", excess atomic hydrogen diffuses out of the catalytic metal into surrounding carbon material, altering its electrical properties.[15,16] The physical process(es) involved following hydrogen spillover into carbon materials are still debated.[15] Several authors have attributed sensing responses (in which the resistance of carbon films increases upon exposure to hydrogen) to bonding changes in the carbon. In particular, hydrogenation of dangling carbon bonds and/or sp^2 to sp^3 transitions have been suggested as they are likely to result in altered electrical conductance. However, some reports have cast doubt on the spillover mechanism,[17] stating that hydrogen absorption into carbon materials is energetically unfavorable and therefore unlikely to account for significant changes in the resistance of conductometric carbon hydrogen sensors.

In this paper, we deposit conducting carbon films energetically from a plasma and investigate their response to hydrogen gas. The deposition conditions were selected to produce oriented graphitic films.[11] The effect of nanostructure has been explored by comparing sensors based on films with different degrees of crystalline order. Measurements have also been performed using different sensor designs to help understand the mechanism behind electrical conductivity changes occurring during hydrogen exposure.

Experimental

The carbon films were prepared using a dual bend filtered cathodic arc[18] deposition system operating with a 99.9% pure graphite target, an arc current of 56 A and a base pressure less than 10^{-5} Torr. Insulating quartz substrates were ultrasonically cleaned in acetone and ethanol before being dried and mounted on a substrate heater/holder within the deposition chamber. A regulated DC power supply was connected to a stainless steel mesh placed 12 mm in front of the quartz substrate. A bias voltage of −1000 V was applied to the mesh, enabling the average deposition energy to be increased.[19] Films were prepared using this mesh bias at temperatures of 100 °C and

School of Applied Sciences, RMIT University, GPO Box 2476V, 3001, Melbourne, Australia. E-mail: jim.partridge@rmit.edu.au; Fax: +61 3 9925 5290; Tel: +61 3 9925 2865

600 °C. A tetrahedral amorphous carbon (ta-C) layer required for electrical insulation was also deposited using the filtered cathodic arc, with substrate bias/temperature −75 V/30 °C.[11]

The nanostructure of the films was initially analyzed using Raman spectroscopy. A Renishaw In Via system operating with an excitation wavelength of 514 nm and a grating of 2400 lines per mm was used to collect spectra. Imaging of the films was performed using a JEOL 2010 transmission electron microscope (TEM) operating at 200 kV. Electron energy loss spectroscopy (EELS) analysis was performed using a Gatan Imaging Filter (GIF2000). An EELS spectrum was collected in the low loss region in order to determine the plasmon peak position, used to calculate the film density (assuming carbon has four valence electrons with an effective mass of $0.88m_e$ taking part in plasmon oscillations).[20] EELS spectra were also collected in the region of the carbon K-shell ionization edge enabling an estimate of the fraction of sp^2 bonded carbon atoms in each film.[21]

The sensor designs used are shown schematically in Fig. 1. Au electrical contact pads were thermally evaporated onto the carbon films whilst the Pt catalytic metal pads were sputtered. The contacts at the ends of the film were approximately 2 × 2 mm^2 and the central catalytic pads were approximately 2 × 4 mm^2. The insulating ta-C layer incorporated into the 'type C' design measured approximately 20 nm in thickness and 3 × 5 mm^2 in area. A stencil was used to define the dimensions of all contacts during their deposition.

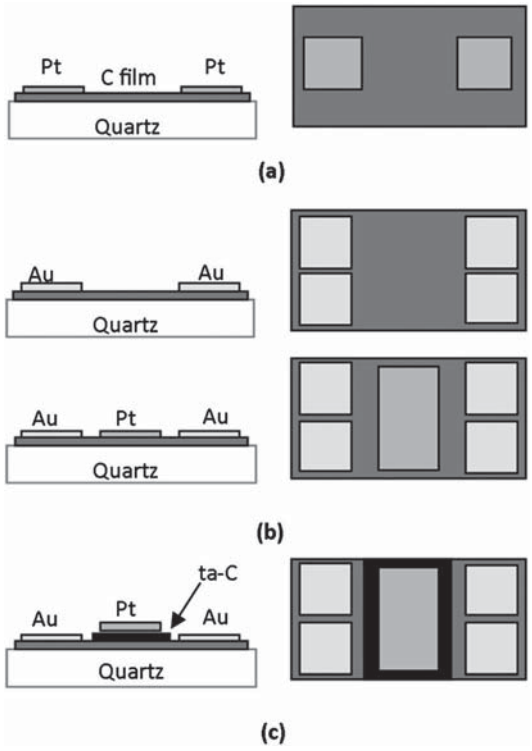

Fig. 1 Cross-sectional (left) and plan view (right) representations of the (a) 'type A', (b) 'type B' and (c) 'type C' conductometric hydrogen gas sensors incorporating oriented carbon films. Note that the type B sensor was fabricated with and without a central catalytic Pt pad and the Pt pad in the type C sensor is electrically isolated from the oriented carbon beneath using a tetrahedral amorphous carbon layer.

The sensing measurements were performed using a multi-channel gas test chamber. Computer interfaced mass flow controllers were used to expose the sensors to concentrations of hydrogen gas from 0.125% to 1%. Au wires were bonded onto the contacts using conductive silver-paint. This silver paint was tested independently to verify that it exhibited no electrical response during exposure to hydrogen gas. Four-probe and two-probe electrical measurements were performed using a computer interfaced multimeter and source-meter. The total gas flow rate was maintained at 200 sccm and the reference gas was synthetic air (certified zero humidity).

Results and discussion

Fig. 2 shows the Raman intensity in the 1000 to 1800 cm^{-1} region from the films deposited using mesh bias at both low and high temperature. Also shown for comparison is the Raman spectrum for glassy carbon heat treated to 3000 °C. Glassy carbon has a microstructure consisting of cross-linked graphite-like ribbons 3–4 nm in width.[22] The Raman spectrum in this spectral region is mainly sensitive to in-plane vibrational modes of the sp^2 bonded component.[23] The major features are the so called graphite or 'G' peak at 1580 cm^{-1}, corresponding to the zone center E_{2g} Raman active mode of graphite,[24] and the disorder or 'D' peak at 1355 cm^{-1}, corresponding to a feature in the vibrational density of states of layered sp^2 structures.[24] The Raman spectrum for the film prepared at low temperature shows both the D and G peaks, indicating that the microstructure of the film is largely graphitic. However, both peaks are broader than those observed in glassy carbon, indicating that the graphitic layers have higher defect densities. Both the D and G peak become sharper in the film prepared at higher

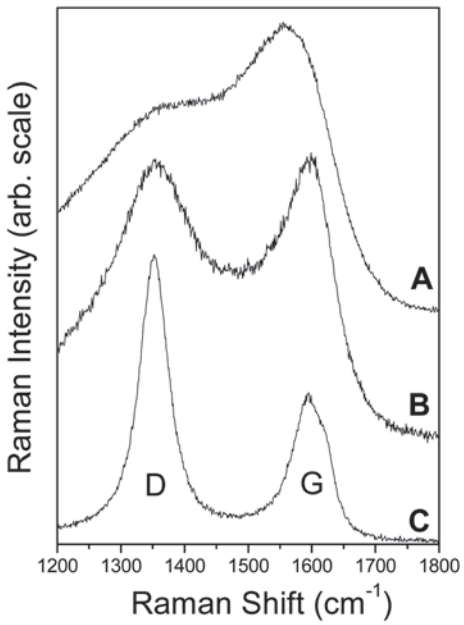

Fig. 2 The Raman spectrum of the carbon films prepared on quartz at temperatures of (A) 100 °C and (B) 600 °C. Included is (C) the Raman spectrum from a bulk sample of glassy carbon heat treated to 3000 °C showing the characteristic D and G peaks produced by disordered graphitic materials.

temperatures indicating a higher degree of in-plane graphitic order. Note that the Raman spectra from all samples is unlike that of typical amorphous carbon films which consist of a broad asymmetric line shape centered at about 1570 cm^{-1}.[25]

Fig. 3 shows plan view TEM images of films deposited using mesh bias at both low and high temperature. Diffraction patterns (insets in each image) show rings that have been indexed to graphite and provide evidence of preferred orientation. The film deposited at low temperature (Fig. 3(a)) is disordered but includes small graphitic regions, consisting of a small number of parallel graphitic {002} planes. The application of both high bias and high temperature (600 °C) results in a more ordered graphitic microstructure with the graphitic regions extending throughout the plan view TEM image shown in Fig. 3(b). This graphitic nanostructure has been observed previously in carbon films deposited onto conducting substrates with bias applied directly.[12]

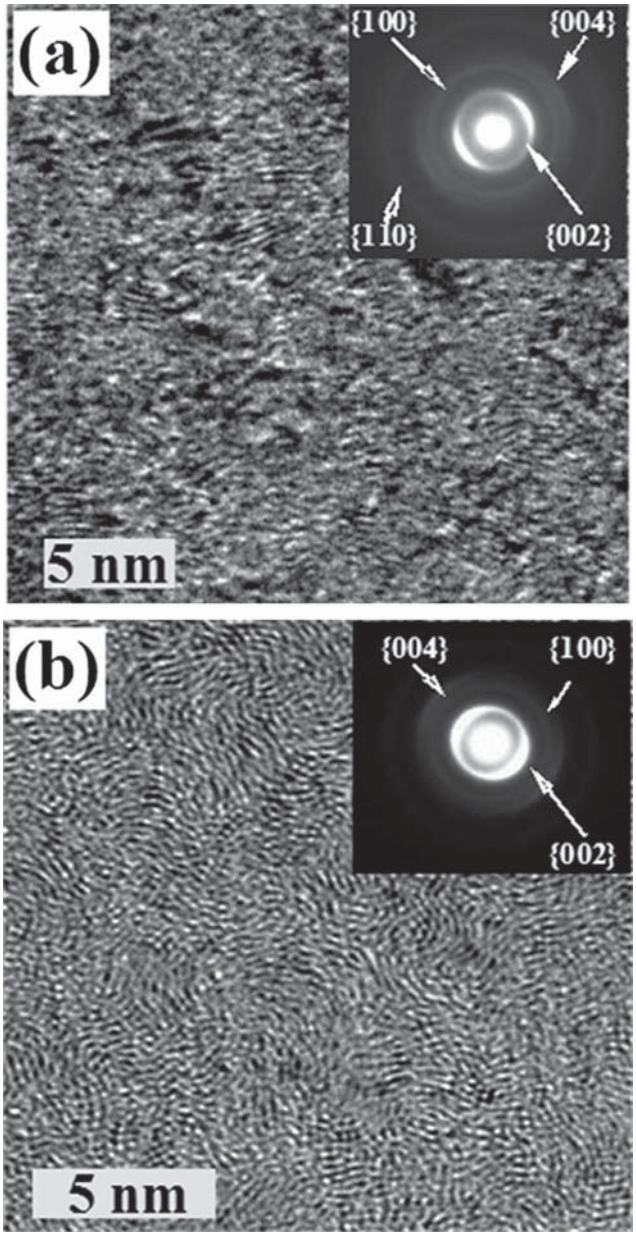

Fig. 3 TEM images of oriented carbon films prepared at (a) low and (b) high temperatures. The inset in each image is an electron diffraction pattern indexed to graphite.

Fig. 4 shows the carbon K edges from both oriented carbon films and glassy carbon. The spectra reflect the unoccupied density of states in the material with a sharp peak at approximately 285 eV corresponding to transitions of carbon 1s electrons to unoccupied π states (labeled 1s to π^*) and a broader feature centered at 300 eV, resulting mainly from 1s to σ^* transitions. In the glassy carbon (labeled C in Fig. 4), the 1s to π^* peak is sharp and the 1s to σ^* feature has fine structure at approximately 292 eV. Both of these features are consistent with the presence of well-ordered graphitic layers. The spectra from the carbon film grown at low temperature (labeled A in Fig. 4) shows a less intense 1s to π^* peak and a broad 1s to σ^* feature. This is consistent with an increase in disorder present in this film compared with glassy carbon. The spectra from the film prepared at high temperatures (labeled B in Fig. 4) is similar to that obtained from glassy carbon indicating that their microstructures are similar. However, the slightly broader features indicate a higher degree of disorder. The sp^2 bonding fractions calculated using the 1s to π^* features were 0.6 ± 0.1 and 0.8 ± 0.1 in the low and high temperature films, respectively. The corresponding film densities were estimated to be 2.3 ± 0.1 and 2.1 ± 0.1 g cm^{-3} from the position of their EELS plasmon peaks (not shown), consistent with previous density measurements from oriented carbon films.[12]

The normalized changes in resistance measured from type A sensors are shown in Fig. 5. The response of the sensor formed on the carbon film deposited at low-temperatures to various concentrations of hydrogen gas in air at 120 °C is shown in Fig. 5(a). The resistance decreased by approximately 10% during exposure to 1% hydrogen in air. The response and recovery times at this exposure level were 1.5 min and 1.7 min, respectively. These times compare very favorably with those reported

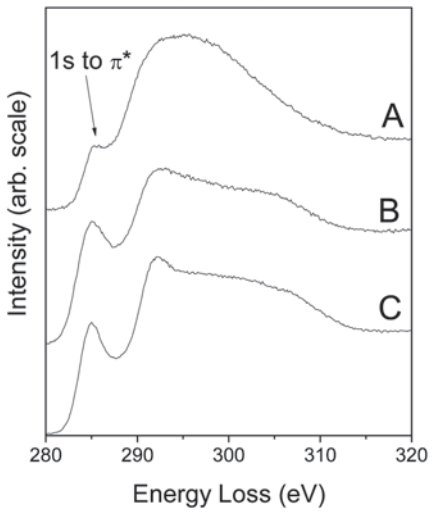

Fig. 4 Carbon K edges from oriented carbon films grown at (A) low temperature (B) high temperature and (C) a bulk glassy carbon sample.

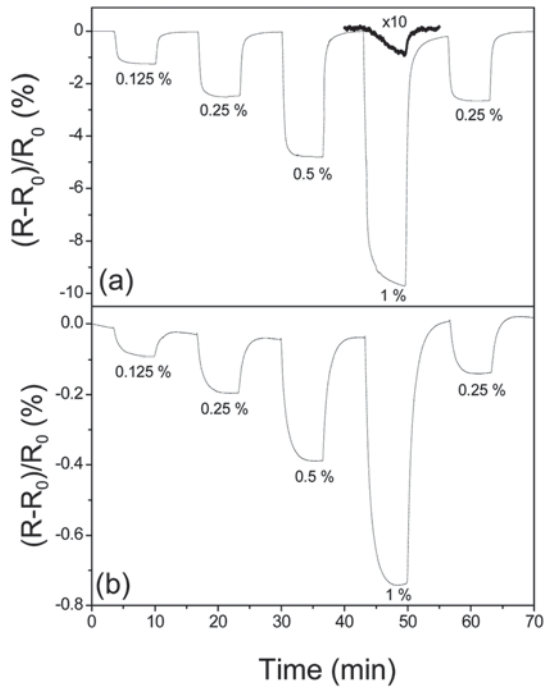

Fig. 5 The normalized change in resistance during the exposure to the indicated concentrations of hydrogen in synthetic air in type A sensors at 120 °C made from (a) low and (b) high temperature carbon films. Also shown in (a) is the response of this sensor at room temperature (thick solid line) to 1% hydrogen magnified by a factor of 10.

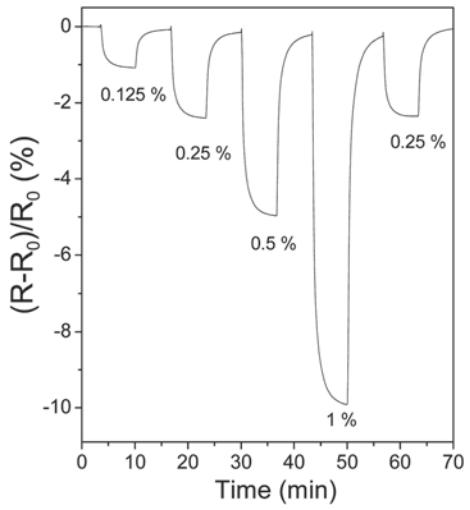

Fig. 6 The normalized change in resistance upon exposure to the indicated concentrations of hydrogen in synthetic air measured from the type B sensor at 120 °C with a central Pt pad and made using the low temperature carbon films. Note that this measurement was made in two-probe configuration using a single contact at each end of the sensor.

for sensors based on other carbon materials including carbon nanotubes.[9] Fig. 5(b) shows the corresponding results for the film prepared at higher temperature. The maximum normalized resistance decrease during exposure to 1% hydrogen in air was less than 1%. This suggests that the increased graphitic order in the film results in a weaker interaction with hydrogen.

The response to hydrogen of both sensors was also measured at room temperature. A very weak and slow response to 1% hydrogen gas in air was observed only from the low temperature deposited film and is shown (thick solid line) in Fig. 5(a). This temperature dependent response strongly suggests that catalytic action is required to produce a sensing response.

The type B sensors, consisting of non-catalytic Au contact pads with and without a central non-contacted catalytic Pt pad, were employed to assess the role of the catalyst in the overall response of the sensors. Gas sensing measurements were first performed on type B sensors with no Pt catalytic pad and no responses were observed. This confirmed that the sensing response demonstrated in the type A sensors relied upon the presence of the catalytic Pt. Previous investigations have also shown that conductometric hydrogen sensors fabricated using carbon based materials require the presence of a catalytic metal to produce measurable responses.[4] Importantly, this indicates that atomic hydrogen caused the decrease in the resistance of the type A sensor.

Fig. 6 shows the responses of type B sensors formed on the low-temperature deposited carbon film including a central Pt pad. This measurement was made in two-probe configuration using a single contact at each end of the sensor. This result is almost identical to that obtained from the type A sensor (Fig. 5(a)) made from the same film, once again confirming that a response occurs only when atomic hydrogen is created by the catalytic Pt.

As stated in the introduction, the response in a conductometric hydrogen sensor can be due to changes in bulk carrier concentration and/or changes in the electrical characteristics of the contact interfaces. For example, in metal–oxide thin film sensors, differences in work functions frequently occur at the contact/film interfaces, resulting in potential barriers with widths that are modulated during hydrogen exposure.[26] Room temperature and 120 °C two-probe current–voltage measurements taken from the Au contacts in these sensors showed Ohmic behavior and indicated that in air or during hydrogen exposure no significant potential barriers existed. Previous electrical measurements performed on oriented carbon films deposited onto p-type silicon and using metallic contacts also exhibited Ohmic behavior.[11]

In order to determine whether the resistance decrease observed upon hydrogen exposure occurs as a result of changes in the electrical characteristics of the contact interfaces in the type B sensors, four-probe measurements were also performed. These were conducted at 120 °C and room temperature in air and during hydrogen exposure by measuring the potential difference between two contacts whilst driving a current through another two contacts (see Fig. 1(b)). The response measured in this way was identical to that measured using the two-probe configuration, showing that the measured responses were primarily due to changes in the electrical resistivity of the carbon films. The possibility that the observed responses to hydrogen occurred due to either volumetric changes in the Pt pads or changes in the resistance of the Pt were discounted using the 'type C' conductometric sensor (shown in Fig. 1(c))

featuring an electrically isolated catalytic Pt pad. The electrical resistance of this sensor decreased by approximately 6% during exposure to 1% hydrogen gas in air at 120 °C, confirming that the response did not occur due to structural/electrical changes in the Pt pad. Electrical isolation of the Pt pad was confirmed by probes and current–voltage measurements in air and during hydrogen exposure.

Our results can be explained by the hydrogen spillover effect[15] in which atomic hydrogen is generated in a catalyst and subsequently diffuses to the supporting material. Experimental studies have shown that atomic hydrogen diffusing in carbon materials can form C–H bonds at moderate temperatures.[27,28] The Raman measurements (Fig. 2) showed that both oriented carbon films contain a significant number of defects. Since the film containing the higher number of defects exhibited a larger response to hydrogen, we believe that atomic hydrogen either bonds to these defect sites or alters them, leading to changes in their electrical characteristics. The rapid recovery of the sensors in air shows that these changes are reversible and that any hydrogen bonding is weak.

Disordered graphitic materials, with similar nano-structure to the films described here, demonstrate resistance that decreases with temperature and are therefore frequently described as semiconductors.[22,29] This semiconducting behavior originates by virtue of stable defects that raise barriers against charge carrier transport.[22] Bulk disordered graphitic carbons can exhibit n- or p-type electrical characteristics depending on their degree of crystallographic order, controlled by the growth/annealing temperature.[22,29] Defects having donor or acceptor like character are removed and created at different growth/annealing temperatures, explaining the complex behavior of the Hall coefficient.[22] Since the resistance of all the carbon films tested decreased upon exposure to hydrogen, an increase in the carrier concentration or an increase in the mobility must occur due to the hydrogen bonding. Hot probe electrical measurements[30] performed on both carbon films revealed that the dominant carriers were holes and the films were therefore p-type. We believe that spilt-over atomic hydrogen, diffusing in the oriented carbon films, is likely to form metastable bonds to defect sites, leading to the creation of more acceptor states and/or an increase in carrier mobility. This results in the observed reduction in resistance during hydrogen exposure. These bonds are weak and once the supply of hydrogen is removed, the number of hydrogen atoms bonded to defect sites within the carbon structure reduces rapidly resulting in an increase in resistance back to its original level.

Conclusions

The electrical resistance of oriented carbon films has been measured in air and during exposure to hydrogen gas in air. The resistance decreased only when catalytic Pt pads were attached to the carbon films. Four-probe electrical measurements confirmed that the resistance of the carbon film decreased in the presence of hydrogen and contact effects were negligible. The sensitivity of the sensor to hydrogen was found to depend on the degree of crystallographic order within the film, indicating that defects were critical to the response mechanism. The mechanism for gas sensing was attributed to hydrogen spillover from the catalytic Pt pad into the underlying carbon film. The hydrogen diffuses through the carbon structure forming weak bonds to defect sites which leads to changes in the electrical resistance of the oriented carbon material.

Acknowledgements

The authors would like to thank Jennifer Hartley from the Industrial Research Institute at Swinburne University of Technology for assistance with the Raman spectroscopy and the RMIT University Microscopy and Microanalysis Facility. The authors also gratefully acknowledge the Australian Research Council for financial support.

Notes and references

1 A. C. Dillon and M. J. Heben, *Appl. Phys. A: Mater. Sci. Process.*, 2001, **72**, 133–142.
2 J. Li, Carbon-based Sensors, in *Carbon Materials for Catalysis*, ed. P. Serp and J. L. Figueiredo, John Wiley & Sons Inc., USA, 2008, ch. 14.
3 J. Kong, M. G. Chapline and H. Dai, *Adv. Mater.*, 2001, **13**, 1384–1386.
4 M. K. Kumar and S. Ramaprabhu, *J. Phys. Chem. B*, 2006, **110**, 11291–11298.
5 F. Schedin, A. K. Geim, S. V. Morozov, E. W. Hill, P. Blake, M. I. Katsnelson and K. S. Novoselov, *Nature*, 2007, **6**, 652–655.
6 S. G. Wang, Q. Zhang, D. J. Yang, P. J. Sellin and G. F. Zhong, *Diamond Relat. Mater.*, 2004, **13**, 1327–1332.
7 J. Zhao, A. Buldum, J. Han and J. Ping Lu, *Nanotechnology*, 2002, **13**, 195–200.
8 L. Valentini, C. Cantalini, I. Armentano, J. M. Kenny, L. Lozzi and S. Santucci, *Diamond Relat. Mater.*, 2004, **13**, 1301–1305.
9 J. Sippel-Oakley, H.-T. Wang, B. S. Kang, Z. Wu, F. Ren, A. G. Rinzler and S. J. Pearton, *Nanotechnology*, 2005, **16**, 2218–2221.
10 Ph. Avouris, T. Hertel, R. Martel, T. Schmidt, H. R. Shea and R. E. Walkup, *Appl. Surf. Sci.*, 1999, **141**, 201–209.
11 D. W. M. Lau, D. G. McCulloch, M. B. Taylor, J. G. Partridge, D. R. McKenzie, N. A. Marks, E. H. Teo and B. K. Tay, *Phys. Rev. Lett.*, 2008, **100**, 176101.
12 D. W. M. Lau, A. Moafi, M. B. Taylor, J. G. Partridge, D. G. McCulloch, R. C. Powles and D. R. McKenzie, *Carbon*, 2009, **47**, 3263–3270.
13 C. Lin, Z. Yang, T. Xu and Y. Zhao, *Appl. Phys. Lett.*, 2008, **93**, 23110.
14 K. Tsukada, T. Kiwa, T. Yamaguchi, S. Migitaka, Y. Goto and K. Yokosawa, *Sens. Actuators, B*, 2006, **114**, 158–163.
15 G. M. Psofogiannakis and G. E. Froudakis, *Chem. Commun.*, 2011, **47**, 7933–7943.
16 L. Chen, A. C. Cooper, G. P. Pez and H. Cheng, *J. Phys. Chem. C*, 2007, **111**, 18995–19000.
17 R. Prins, *Chem. Rev.*, 2012, **112**, 2714–2738.

18 A. Anders, *Cathodic Arcs: From Fractal Spots to Energetic Condensation*, Springer, USA, 2008.
19 A. Moafi, D. W. M. Lau, A. Z. Sadek, J. G. Partridge, D. R. McKenzie and D. G. McCulloch, *J. Appl. Phys.*, 2011, **109**, 073309.
20 R. F. Egerton, *Electron Energy-Loss Spectroscopy in the Electron Microscope*, Plenum/Springer, New York, 2nd edn, 1996.
21 S. D. Berger, D. R. McKenzie and P. J. Martin, *Philos. Mag. Lett.*, 1988, **57**, 285–290.
22 G. M. Jenkins and K. Kawamura, *Polymeric Carbons – Carbon, Fibre Glass and Char*, Cambridge University Press, Cambridge, 1976.
23 C. Z. Wang and K. M. Ho, *Phys. Rev. Lett.*, 1993, **71**, 1184–1187.
24 R. Al-Jishi and G. Dresselhaus, *Phys. Rev. B: Condens. Matter Mater. Phys.*, 1982, **26**, 4514–4522.
25 R. O. Dillon, J. A. Woollam and V. Katkanant, *Phys. Rev. B: Condens. Matter Mater. Phys.*, 1984, **29**, 3482–3489.
26 E. Comini, *Anal. Chim. Acta*, 2006, **568**, 28–40.
27 A. Nikitin, H. Ogasawara, D. Mann, R. Denecke, Z. Zhang, H. Dai, K. Cho and A. Nilsson, *Phys. Rev. Lett.*, 2005, **95**, 225507.
28 A. Nikitin, X. Li, Z. Zhang, H. Ogasawara, H. Dai and A. Nilsson, *Nano Lett.*, 2008, **8**, 162–167.
29 I. L. Spain, in *Chemistry and Physics of Carbon*, Dekker, New York, 1981, vol. 16, pp. 119–304.
30 L. E. J. Cowles and L. A. Dauncey, *J. Sci. Instrum.*, 1962, **39**, 16–18.